DOI:10.28974/idojaras.2021.2.1

IDŐJÁRÁS

Quarterly Journal of the Hungarian Meteorological Service
Vol. 125, No. 2, April – June, 2021, pp. 167–192

Local identification of persistent cold air pool conditions in the Great Hungarian Plain

Karolina Szabóné André [1,2,*], **Judit Bartholy** [1], **Rita Pongrácz** [1], and **József Bór** [2]

[1] *Department of Meteorology*
Eötvös Loránd University
Pázmány Péter st. 1/A, H-1117, Budapest, Hungary

[2] *Institute of Earth Physics and Space Science (ELKH EPSS)*
Csatkai Endre st. 6-8, H-9400, Sopron, Hungary

**Corresponding author E-mail: karol@nimbus.elte.hu*

(Manuscript received in final form April 28, 2020)

Abstract— Cold air pool (CAP) is a winter-time, anticyclonic weather event: a cold air layer confined by the topography and warm air aloft. If its duration is more than one day, then it is called persistent cold air pool (PCAP). CAPs are mainly examined in small basins and valleys. Fewer studies pay attention to PCAPs in much larger basins (with an area of more than 50 000 km^2), and it is not evident how effective the existing numerical definitions are in cases of extensive PCAP events. A possible method of identifying PCAPs in a large basin is to identify PCAP weather conditions at different measuring sites across the basin. If there are PCAP weather conditions at most of the sites, then it is likely to be an extensive PCAP.

In this work, we examine which of the documented CAP definitions can be used for reliable local detection of CAP conditions. Daily weather reports and meteorological data from two locations in the 52 000 km^2 sized Great Hungarian Plain have been used to obtain a reference set of days with PCAP weather conditions during two consecutive winter months. Several numerical CAP definitions were compared for their performance in recognizing the presence of PCAP weather conditions using radiosonde measurements and reanalysis data. The lowest error was produced by using the heat deficit (HD) method. So this is considered the most suitable method for local identification of PCAPs in the Great Hungarian Plain.

Key-words: persistent cold air pool; temperature inversion; heat deficit; Carpathian Basin; radiosonde; reanalysis

1. Introduction

Two very different meteorological phenomena are named cold air pool (CAP) in the literature. One of them is a synoptic scale weather formation, when there is a cold air mass above warmer air causing heavy precipitation (e.g., *Llasat* and *Puigcerver*, 1990). The subject of our study is the second one, which is a stagnant cold air layer in a basin or valley below a warmer air layer (*Whiteman et al*., 2001). This latter phenomenon is anticyclone-related and favorable to fog formation due to the weak near-surface wind and the strong temperature inversion causing limited vertical motion (*Chachere* and *Pu*, 2016). The subsidence in anticyclone plays a key role in the formation of the inversion.

CAPs can be classified into two subgroups based on the height of the base of the inversion: simple or complex (*Tóth*, 1984). In the simple case, the inversion layer starts directly from the surface, and if the level of relative humidity is sufficiently high then fog forms. This stratification can lead to severe smog events in populated areas, where various pollutants are emitted from traffic, industry, and households (e.g., *Deng et al*., 2019). In the complex case, an unstable layer forms near the surface below the temperature inversion. This leads to the formation of elevated fog or stratus cloud if the atmosphere is wet enough. CAPs can transform from simple to complex type and vice versa over time.

CAPs can be classified into two other subtypes according to their duration: nocturnal only or persistent event. Nocturnal CAP usually forms during the night and dissipates after sunrise due to the substantial change in energy budget elements associated to incoming solar radiation. It can occur throughout the year mainly in small valleys or basins (usually in the range of a few 10–100 km^2). Persistent cold air pools (PCAPs) remain longer than a single diurnal cycle and can last several days or even for weeks. More specifically, this weather event typically occurs in winter, because the solar elevation angle is smaller and the daytime is shorter than in summer. These conditions lead to less incoming solar radiation that cannot destroy the inversion layer. The snow cover is also favorable for the inversion development.

PCAPs may result in different socio-economic hazards: temperature inversion in the surface layers together with weak wind may lead to severe air pollution in cities causing health problems for many people, especially, elderly and children even in smaller settlements. For instance, *Largeron* and *Staquet* (2016a) examined the connection between persistent inversions and wintertime PM_{10} pollution in the valleys surrounding Grenoble, France. Their study concluded that polluted episodes are primarily driven by persistent inversions. Fog and/or smog during chilly weather conditions often results in freezing drizzle and rime accretion. These weather conditions can cause problems in transportation and electricity supply. Therefore, CAPs have a significant impact on the daily lives of the population. Unfortunately, simulating CAPs is difficult that causes a large forecasting error in

numerical weather forecasting models near the surface. That is why it is important to find a metric that adequately describes CAPs.

To study the different stages of the life cycle of CAPs in more detail, numerous experiments and field measurement campaigns were performed. In the Stable Atmospheric Boundary-Layer Experiment (SABLES 98), *Cuxart et al*. (2000) examined dynamical processes including winds in the nocturnal stable boundary layers in Spain. They observed low-level jets during every nocturnal CAP. In the Meteor Crater Experiment (METCRAX), *Whiteman et al*. (2008), the effect of solar radiation and winds on CAP evolution was investigated in Arizona, USA. Their preliminary results show that nocturnal CAP forms frequently in the crater, and internal wave motions are common in CAP. During the Cold-Air Pooling Experiment (COLPEX), the formation of CAP and fog was examined within valleys in the United Kingdom (*Price et al.,* 2011). According to the results, the temperature and turbulence during CAPs is generally greater in the Burfield valley than in the less open Duffryn valley. Initial results indicate that when clouds advected over the valley, the stability is greatly reduced. When sky becomes clear, CAP forms again. Numerical modeling of CAPs was also addressed in COLPEX using the data measured during the experiment. The initial results show that some of the successfully simulated CAPs are slightly too cold. The Persistent Cold-Air Pool Study (PCAPS) was performed to get more measurements and better understanding of PCAPs in Utah, USA (*Lareau et al*., 2013). They showed that there is a connection between strong, long lasting PCAPs and high concentration of fine particulate matter.

The wide variety of field campaigns and perspectives led to the use of different numerical definitions. Several definitions are reviewed here only briefly and are described in detail later in Section 3. The earliest study to describe and define CAPs in the intermountain western USA was performed by *Wolyn* and *McKee* (1989). They introduced the concept of deep stable layer (DSL). Later, *Chachere* and *Pu* (2016) also used this definition and referred to the DSL as CAP. *Yu et al.* (2017) also used this method but considered the wind speed at 10 m, too.

Other methods are based on the identification of inversion over a valley or basin. There are different techniques for this purpose, for example the temperature difference between the mountain ridge and the valley base (*Iijima* and *Shinoda,* 2000; *Vitasse et al*., 2017; *Conangla et al*., 2018), or the vertical temperature profile can also be used (*Kahl et al*., 1992). Some authors also include an upper threshold for wind speed because of the typical weak wind conditions during CAP episodes (*Whiteman et al*., 2001; *Reeves* and *Stensrud*, 2009; *Reeves et al*., 2011).

Another group of methods is based on the so-called heat deficit (e.g., *Whiteman et al*., 1999, 2014; *Chemel et al*., 2016; *Largeron* and *Staquet*, 2016a, 2016b; *Baasandorj et al*., 2017). This measure describes the atmospheric stability of an air column.

Lareau et al. (2013) introduced a method based on the potential temperature deficit (PTD) to define CAPs.

CAPs are usually investigated in small basins (few 10–100 km^2), where the approximation of horizontal temperature homogeneity can be used (*Largeron* and *Staquet*, 2016a). In this case, even a single measurement site that monitors the vertical temperature profile is sufficient to identify PCAPs. Fewer studies pay attention to PCAPs in much larger basins with an area of more than 50 000 km^2, like, e.g., the Colorado Plateau Basin of size 225 000 km^2 (*Whiteman et al*., 1999). Consequently, it is not evident how effective the existing numerical definitions are in cases of extensive CAP events. A possible method for identifying PCAPs in a large basin is to identify PCAP weather conditions at different measuring sites across the basin. If there are PCAP weather conditions at most of the sites, then it is likely an extended PCAP. The extension of the event can be estimated considering the areal coverage of stations.

In our study, weather conditions are analyzed in the 52 000 km^2 sized Great Hungarian Plain, and two locations (Budapest and Szeged, Hungary) with radiosonde measurements are considered to test local identification of PCAP weather conditions during two consecutive winter months (December 2015 and January 2016). The above-mentioned numerical CAP definitions are compared for their performance in recognizing the presence of PCAP weather conditions near these two cities.

A suitable numerical definition could be utilized possibly in synoptic-climatological research and air quality studies (e.g., *Haszpra et al*., 2019) as well as by weather forecasters during post-processing of numerical weather prediction models.

2. Data

The two considered measuring stations (Budapest and Szeged) can be found in the Carpathian Basin, which is located in Central Europe (*Fig. 1*) surrounded by the Alps (from west), the Carpathian Mountains (from north, east, and south) and the Dinarides (from south). The general altitude of the Carpathian Mountains is around 1500 m, with several peaks above 2000 m. The average height of 850 hPa pressure level is 1500 m, therefore, this level has a prominent role in this study.

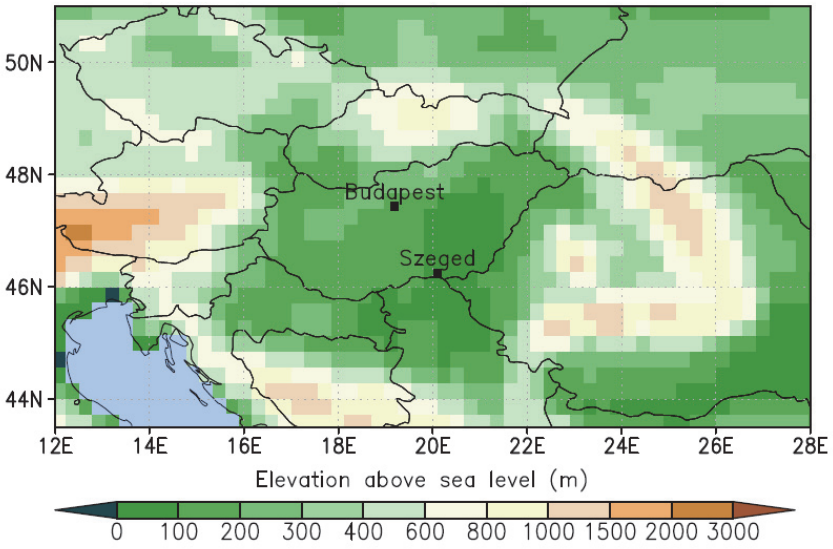

Fig. 1. Topography of the Carpathian Basin and its surroundings from the ERA5 reanalysis dataset with a horizontal resolution of 0.28125° (~31 km). The examined locations are indicated with black dots: Budapest and Szeged in Hungary.

The Integrated Global Radiosonde Archive (IGRA) database (*Durre et al.*, 2006; IGRA dataset) was used to examine PCAPs. There were two measurements in a day during the examined period of two months. Only one measurement is missing at Budapest, namely, on December 11, 2015 at 12 UTC.

Surface synoptic reports from the Integrated Surface Dataset (ISD) (*Smith et al.*, 2011; ISD dataset) were used for describing the weather conditions of the examined months at Budapest and Szeged. The following variables are used from the reports: hourly atmospheric pressure at station level, temperature and dew point temperature at 2 m, and wind speed at 10 m. There are 28 and 50 missing measurements at Budapest and Szeged, respectively. Out of them, 8 and 20 correspond to 00 UTC or 12 UTC, when radiosonde measurements are regularly available.

To obtain finer temporal resolution, two global gridded reanalysis datasets were used: the ERA-Interim (with ~79 km horizontal resolution, *Dee et al.,* 2011; ERA-Interim dataset) and the ERA5 (with ~31 km horizontal resolution, *Hersbach et al.*, 2019; ERA5 dataset). These datasets are available with temporal resolutions of 6 h and 1 h, respectively. Main technical details of the databases used in this study are summarized in *Table 1*. For the present analysis, we used only the data from the two grid cells containing the measuring sites.

Table 1. Technical details of databases used in this study to examine PCAPs

		IGRA	ISD	ERA-Interim	ERA5
Data type		measurements	measurements	reanalysis	reanalysis
Horizontal resolution		station data	station data	~79×79 km^2	~31×31 km^2
Temporal resolution (h)		12	1	6	1
Stations/grid cell center coordinates and elevation above mean sea level	**Budapest, Hungary**	47.4333°N 19.1833°E 138 m	47.4333°N 19.1833°E 138 m	47.25°N 19.5°E 126 m	47.53156°N 19.12533°E 168 m
	Szeged, Hungary	46.25°N 20.1°E 82 m	46.25°N 20.1°E 82 m	46.5°N 20.25°E 80 m	46.1254°N 19.9688°E 90 m
Number of vertical pressure levels below 850 hPa (including 850 hPa)		variable (min.: 3, max.: 11, average: 7)	surface data	7	7
Missing data		Szeged: 0 Budapest: 1 (12 UTC 11th December 2015)	Szeged: 50 Budapest: 28	None	None

3. Methods

3.1. Producing the reference set of PCAP days

The Daily Weather Reports (DWR website) is a regular product of the Hungarian Meteorological Service (HMS) prepared by experienced synoptic meteorologists. This document describes the European and Hungarian weather situation every day. It contains a map with weather fronts and cloud cover over Europe and some maps with measured data from several locations in Hungary (e.g., daily maximum and minimum temperature, calculated sunshine duration, amount and type of precipitation, maximum wind gust).

In addition to DWR, radiosonde measurements were also used to create a reference set of PCAP days. The main criterion for a PCAP day was the presence of a strong, low level inversion above the measuring station throughout the day (from 00 UTC to the subsequent 00 UTC) according to the radiosonde data.

Major steps in determining local reference PCAP days are shown in *Fig. 2*. The presence of mid-latitude cyclone was recognized from the front maps of the

DWR. The presence of the following conditions was examined using the textual report: (1) cumulus clouds, (2) cloudy, foggy weather, and (3) European synoptic situation (warm air advection). The expression "cold air pool" is rarely used in the textual report, but when it is used it always refers to a PCAP. Areas of the stations are identified from context. For example „near the capital", or „central part of Hungary" correspond to Budapest, while „southern part of the country, next to the river Tisza" refers to Szeged.

Producing reference PCAP days data series is a rather time and energy consuming task, and sometimes it is subjective. The benefit of using numerical methods is that objective examinations can be made and they facilitate long-term examinations of PCAPs.

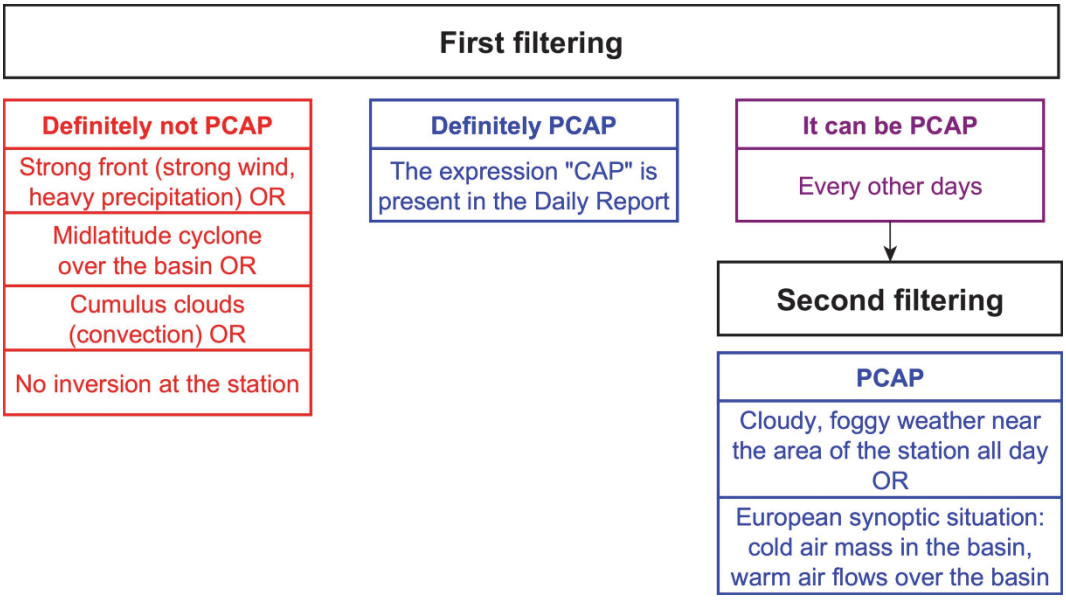

Fig. 2. Major steps in determining local reference PCAP days.

3.2. Persistent temperature inversion

The first numerical method to identify possible PCAP days is based only on atmospheric temperature inversions. To locate the inversion layers, the method designed by *Kahl* (1990) is used. The vertical temperature profile is evaluated from the surface upwards at each location and each time step. The base of a specific inversion is that vertical level where the temperature begins to increase with height for the first time (starting from the surface), while the top of this inversion is that level where temperature begins to decrease with height. If there are more than one inversion layers above each other separated by thin (less than

100 m thick) unstable layer(s), then it is considered as one inversion with embedded unstable layer(s). Inversions thinner than 20 m and inversions with a base above 850 hPa pressure level (i.e., at the general altitude of the Carpathian Mountains) are excluded from the further analysis. If the identified inversion is present all day (i.e., from 00 UTC to the following 00 UTC) according to the available data, then that particular day was taken as a day of persistent inversion. This definition is abbreviated and called INV hereafter.

3.3. Temperature inversion with low wind speed

The second applied definition is the same as INV, but it also considers wind speed at 10 m. If there is inversion and the instantaneous wind speed is lower than 3.1 ms^{-1} (*Whiteman et al.*, 2001) during the whole day (from 00 UTC to the subsequent 00 UTC), then it is defined as a PCAP day. This method is called INV+WSPD.

Wind speed of the lowest level from radiosonde data was used as "10 m wind speed" because of the large number of missing data in ISD (see Section 2). Namely, calculating PCAP days using IGRA combined with ISD data results in 35% missing data in the time series, which would make the comparison with other methods and databases difficult. That is why we used only IGRA data with this method.

3.4. Heat deficit

The third definition is based on the heat deficit (HD, Eq. (1)). HD indicates the energy that is needed for the lapse rate to change to dry adiabatic within an atmospheric column with a 1 m^2 base from the surface to a specific height (*Whiteman et al.*, 2014). The height of the 850 hPa pressure level (see Section 2) was used as a reference. The following formula was used to calculate HD as a function of time:

$$HD(t) = \frac{c_{pd}}{g} \int_{850\ hPa}^{p_0} [\theta_{850hPa}(t) - \theta(p,t)]dp \quad [J\ m^{-2}], \qquad (1)$$

where c_{pd} is the specific heat capacity at constant pressure for dry air (1005 $Jkg^{-1}K^{-1}$), g is the gravitational acceleration (9.81 ms^{-2}), p_0 is the pressure at the lowest level (e.g., surface), $\theta_{850hPa}(t)$ and $\theta(p,t)$ are the potential temperatures at 850 hPa and at a given p level, respectively. The integral part in Eq. (1) is equivalent to the shaded area between the potential temperature profile and the dry adiabatic curve in *Fig. 3*.

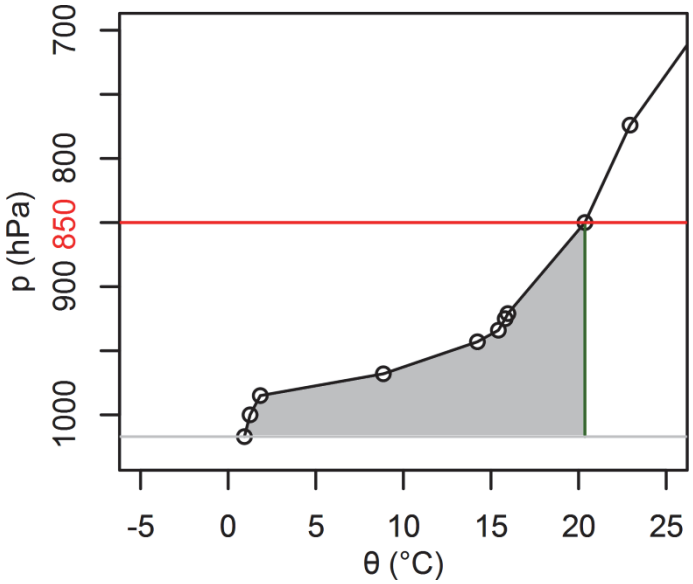

Fig. 3. Illustration of heat deficit using the potential temperature profile (line with circle symbols) at Budapest, 12 UTC, December 26, 2015. The dry adiabatic curve (vertical line) used for HD calculation is also indicated. HD = $c_p/g \times$ shaded area = 13.9 MJm^{-2}.

If the value of HD exceeds 6.56 MJm^{-2} during the whole day (from 00 UTC to the subsequent 00 UTC), then it is considered as a PCAP-like day at the given location. The threshold is defined heuristically by minimizing the total error (see Section 3.7, *Fig. 5*). The short name of this definition is HD6.56.

3.5. Potential temperature deficit

Besides inversion-based and HD-based definitions, potential temperature deficit (PTD; *Lareau et al*., 2013) is also used to identify PCAP-like weather situations. Potential temperature is calculated at all vertical levels using atmospheric temperature (Eq. (2)):

$$\theta_i(t) = T_i(t)\left(\frac{1000\ hPa}{p_i(t)}\right)^{\frac{R_d}{c_{pd}}}, \tag{2}$$

where $p_i(t)$ is the pressure at a given level i, $T_i(t)$ and $\theta_i(t)$ are the temperature and the potential temperature, respectively, at the given pressure level in kelvin (K). R_d is the specific gas constant of dry air (287 $Jkg^{-1}K^{-1}$), and c_{pd} is the specific heat of dry air under constant pressure (1005 $Jkg^{-1}K^{-1}$).

The potential temperature of the 850 hPa pressure level (see Section 2) is subtracted from the potential temperature of each level to get the PTD at any given level (*Fig. 4*):

$$PTD_i(t) = \theta_i(t) - \theta_{850hPa}(t), \tag{3}$$

where CAP is assumed for vertical levels with PTD_i < -8.58 K. If this condition is fulfilled all day long (from 00 UTC to the subsequent 00 UTC) at least at one vertical level, then it is also considered to be a PCAP-like day at the given location. The threshold is defined heuristically by minimizing total error (see Section 3.8, *Fig. 6*). This definition is called PTD8.58 hereafter.

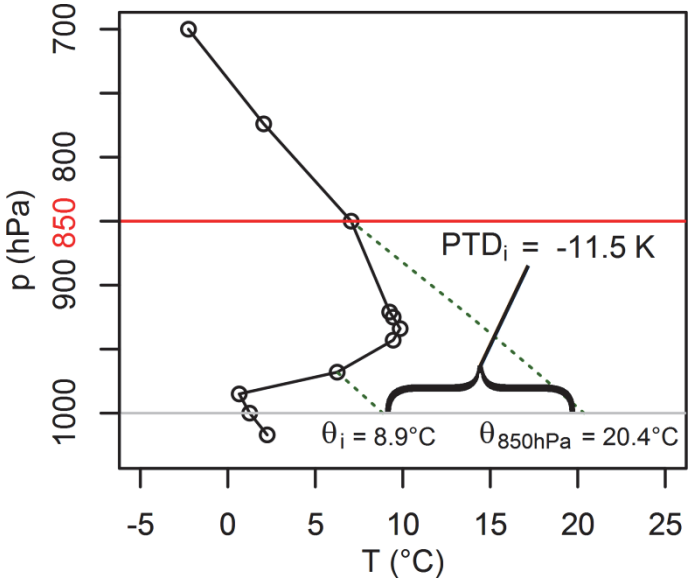

Fig. 4. Illustration of the PTD calculation using the temperature profile (the line with circles indicates the pressure levels of available measurements) at Budapest, 12 UTC, December 26, 2015. Dashed lines indicate dry adiabatic curves used to calculate potential temperatures.

3.6. Evaluating the performance of numerical PCAP identification methods

To compare different numerical PCAP identification methods, three measures derived from the contingency table (*Nurmi*, 2003, Section 4.1) are examined for all of the methods and databases at both stations. The first measure is the probability of false detection (POFD, Eq. (4)) calculated using false alarms and correct rejections (*Table 2*):

$$POFD = \frac{False\ alarms}{False\ alarms + Correct\ rejections}, \tag{4}$$

The second measure is called probability of misses (POM) and calculated as follows (Eq. (5)):

$$POM = \frac{Misses}{Misses + Hits}. \tag{5}$$

Furthermore, the sum of POFD and POM defined as total error (ERR) is evaluated.

Table 2. Contingency table

PCAP-like day according to the numerical method?	**PCAP-like day according to the reference?**	
	Yes	***No***
Yes	Hits (Correct alarms)	False alarms
No	Misses (False rejections)	Correct rejections

3.7. Threshold for the HD-based method

The threshold of HD-based method (see Section 3.4) was determined by calculating ERR with three databases using different thresholds for Budapest and Szeged. *Fig. 5* shows the average ERR (averaging is performed over the databases). The HD threshold values that resulted in the lowest average ERR values are 6.28 MJm^{-2} and 6.84 MJm^{-2} for Budapest and Szeged, respectively. The difference of these values (~8%) is due to the 56 m/46 m/78 m difference in altitude between the two locations using IGRA, ERA-Interim, and ERA5, respectively. The average of the best-performing thresholds for the two cities (6.56 MJm^{-2}) was chosen as a general threshold to identify PCAP days.

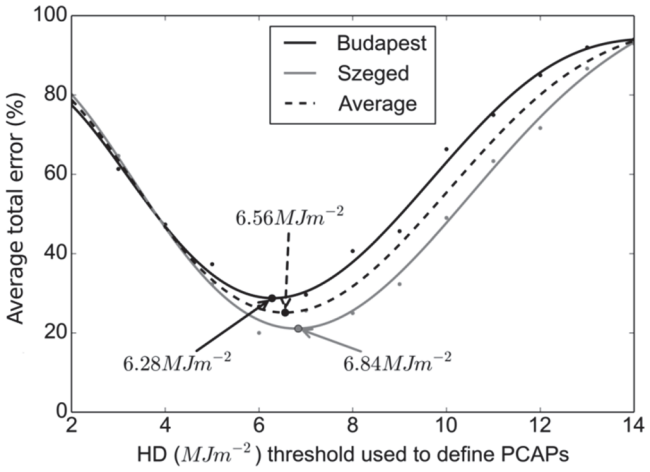

Fig. 5. Determining HD threshold by minimizing the average total error.

3.8. Threshold for the PTD-based method

The threshold of PTD-based method (see Section 3.5) was determined in the same way as in case of HD-based method. The PTD threshold values that resulted in the lowest average ERR values are 8.39 K and 8.86 K for Budapest and Szeged, respectively (*Fig. 6*). The difference of these values (~5%) is due to the 56 m/46 m/78 m difference in altitude between the two locations using IGRA, ERA-Interim, and ERA5, respectively. The average of the best-performing thresholds for the two cities (8.58 K) was chosen as a general threshold to identify PCAP days.

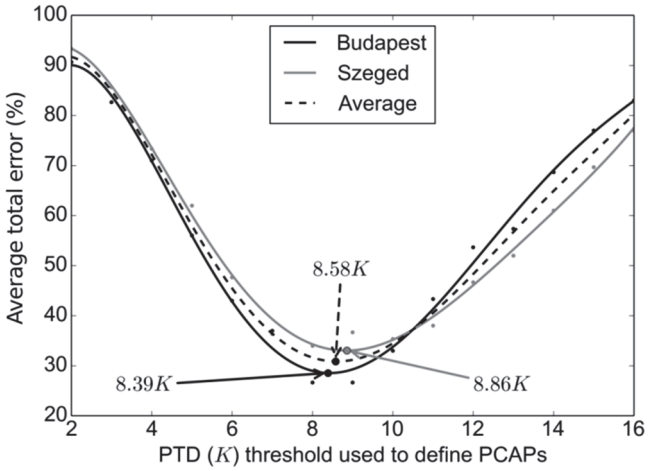

Fig. 6. Determining PTD threshold by minimizing the average total error.

4. Results and discussion

4.1. Weather conditions

Altogether four PCAP events with a duration of 5–17 days occurred over the Carpathian Basin between December 2015 and January 2016 (*Table 3*). The exact dates for the two examined locations were identified (see Section 3.1) and will be used as reference while comparing the definitions described earlier.

Table 3. List of PCAP events between December 2015 and January 2016 over the Carpathian Basin on the basis of Daily Weather Reports of HMS and radiosonde measurements. Non-continuous event means that PCAP conditions were not present within the period up to maximum 1 day

	First day	Last day	Duration (days)	Continuous?
PCAP1	Budapest: December 4, 2015 Szeged: December 5, 2015	December 9, 2015	Budapest: 6 Szeged: 5	yes
PCAP2	December 12, 2015	December 28, 2015	17	yes
PCAP3	January 1, 2016	January 5, 2016	5	yes
PCAP4	January 25, 2016	January 30, 2016	6	no

At the beginning of December 2015, a cold front followed by a warm front passed over the Carpathian Basin. Then, a high-pressure system formed over the basin (*Fig. 7*), and warm air was advected to the area aloft resulting in the formation of PCAP1 on December 4. From that day, anticyclones governed weather across the southern part of Europe, while cyclones were found at the northern part. The Carpathian Basin was located near the border of these areas within the high-pressure part. A cold front brought cold air mass with strong wind on December 10 mixing the air of the basin and destroying the PCAP.

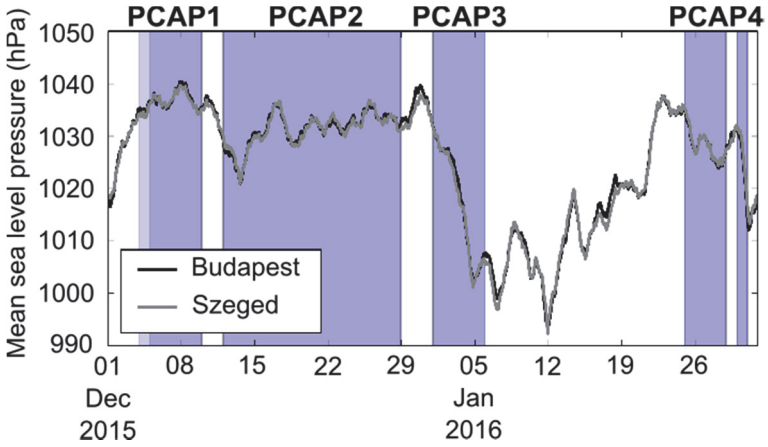

Fig. 7. Mean sea level pressure in Budapest (black) and Szeged (grey) between December 2015 and January 2016. Hourly data are from ISD dataset. Reference PCAP days are also indicated (shaded areas; darker: PCAP present at both stations, light: it is present only at Budapest).

Two days later, the southern anticyclones reached the Carpathian Basin again and PCAP2 formed. The strong westerly wind over Western Europe weakened on

December 27, and the air pressure started to increase over Scandinavia and the Baltic region forming an extended anticyclone. Frosty, dry air mass advected from Siberia at the front side of the high pressure system. It reached the Carpathian Basin on December 29 leading to the dissipation of this PCAP. The temperature decreased by about 10 °C during the following three days (*Fig. 8*).

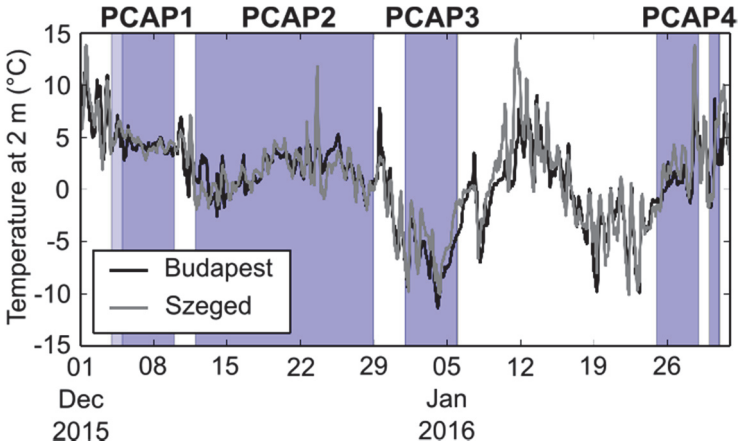

Fig. 8. Temperature at 2 m in Budapest (black) and Szeged (grey) between December 2015 and January 2016. Hourly data are from ISD dataset. Reference PCAP days are also indicated (shaded areas; darker: PCAP present at both stations, light: it is present only at Budapest).

Siberian air filled the Carpathian Basin after the PCAP2 period. Warmer and humid air mass advected over the basin from Western Europe leading to the formation of PCAP3. This event was different from other typical PCAPs. Fog did not occur at the beginning of this event because of the low relative humidity (*Fig. 9*) of the arriving Siberian air mass. In addition to that, the daily maximum speed of wind gusts was below 8 ms^{-1} during PCAP1 and PCAP2, but in this case, it was higher: 8–10 ms^{-1} wind gusts occurred (*Fig. 10*). Also, the air pressure decreased by 30 hPa during PCAP3 to about 1000 hPa (*Fig. 7*). However, PCAPs are usually anticyclonic weather events, so the mean sea level air pressure should be higher than 1013 hPa. According to the maps of the DWR, there was a pressure ridge over the Carpathian Basin during the PCAP3. It means that the pressure was higher in the basin than over some of the neighboring areas. Additionally, the inversion was thick (sometimes more than 1 km) during PCAP3, so the weather inside the basin was quasi-independent from the synoptic weather formations. Considering this situation, the pressure decrease can be understood, if the Mediterranean cyclone passed from west to east near the Carpathian Basin on January 3 is taken into account. Another Mediterranean cyclone with a quite strong warm front passed over the Carpathian Basin on January 6 and led to the dissipation of PCAP3.

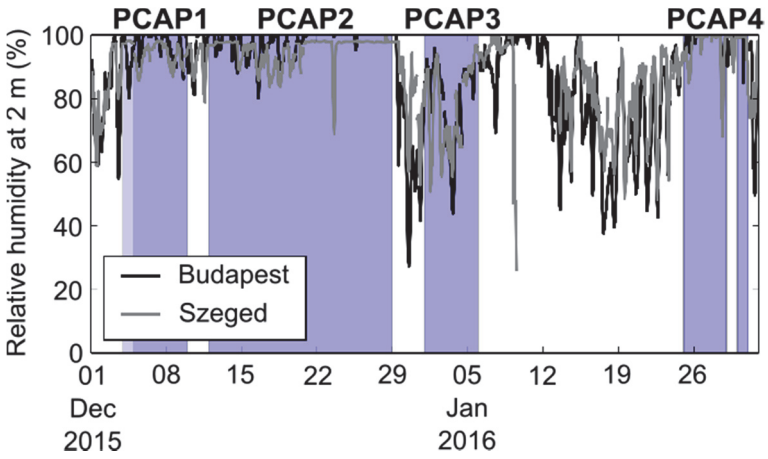

Fig. 9. Relative humidity at 2 m in Budapest (black) and Szeged (grey) between December 2015 and January 2016. Hourly data are from ISD dataset. Reference PCAP days are also indicated (shaded areas; darker: PCAP present at both of the stations, light: it is present only at Budapest).

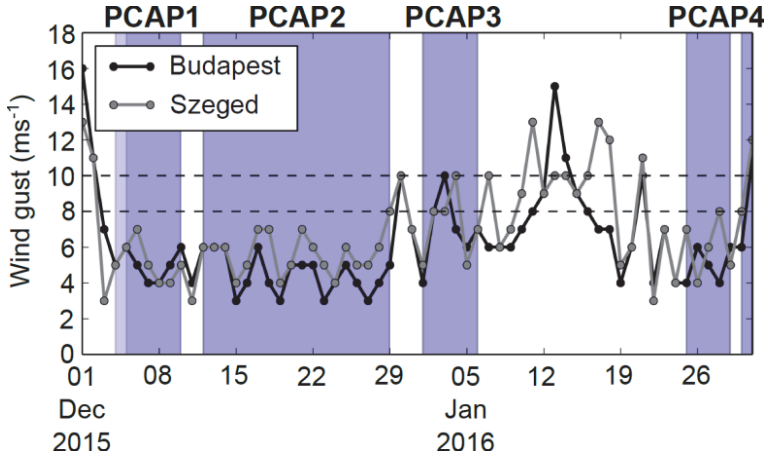

Fig. 10. Daily maximum wind gusts in Budapest (black) and Szeged (grey) between December 2015 and January 2016. Data source: Daily Weather Reports. Reference PCAP days are also indicated (shaded areas; darker: PCAP present at both stations, light: it is present only at Budapest).

A warm front approached the Carpathian Basin on January 8, and the basin was located in the warm sector of a mid-latitude cyclone from 9th to 11th of January. The warm advection caused temperature inversion, which was similar to the inversion during PCAPs. However, this event was definitely not a PCAP but a warm front.

Finally, PCAP4 was formed gradually after a warm front that had passed over the basin on January 23. The inversion strengthened day by day and became a typical PCAP inversion by January 25. Warm air mass advected from west aloft resulting in the changes of the inversion on January 27. It became a lower level inversion and the temperature difference between its base and top strongly increased. A cold front destroyed the PCAP for one day on January 29. Behind the front, the sky was clear and it led to fog formation over large areas during the night of January 29. It means that the PCAP returned within one day. The cold front that passed over the basin on January 31 destroyed this PCAP of short duration.

4.2. Numerical prediction and the reference set of PCAP days

The reference PCAP days between December 1, 2015 and January 31, 2016 summarized for Budapest and Szeged are indicated in the first line of *Fig. 11*. There is some uncertainty in the set of reference PCAP days. On one hand, the names of the cities (Budapest and Szeged) are rarely mentioned in the DWR, so the areas of the stations are identified from context (see Section 3.1). The exact location of the evaluated sites cannot be determined using the DWR. On the other hand, data of the gridded datasets correspond to an exact grid cell. This difference could lead to different results. Furthermore, there are some weather situations that are very complex, e.g., PCAP3 when it is quite challenging to decide whether or not it is a PCAP. In addition to these, it is difficult to determine the exact time of PCAP creation and dissipation, because the DWR is descriptive and the time resolution of IGRA is 12 h. If the inversion is dissipated for 4–7 hours in the afternoon, it cannot be recognized using the radiosonde measurements unlike using reanalyses with 3 h or 6 h temporal resolution. Therefore, it will be defined as PCAP-like day using IGRA, but it will not be defined as PCAP-like day using reanalyses. Note, that thin (< 20 m) inversions can be unambiguously excluded using the radiosonde measurements.

The results for the four numerical PCAP identification methods are also shown in *Fig. 11*. Each method was applied to three databases, which are also indicated at the beginning of the lines. This complex figure can be examined from several points of view. It is possible to compare 1) various numerical methods to the reference, 2) measurement-based results to reanalysis-based results, 3) the two reanalyses, 4) results from individual stations to each other.

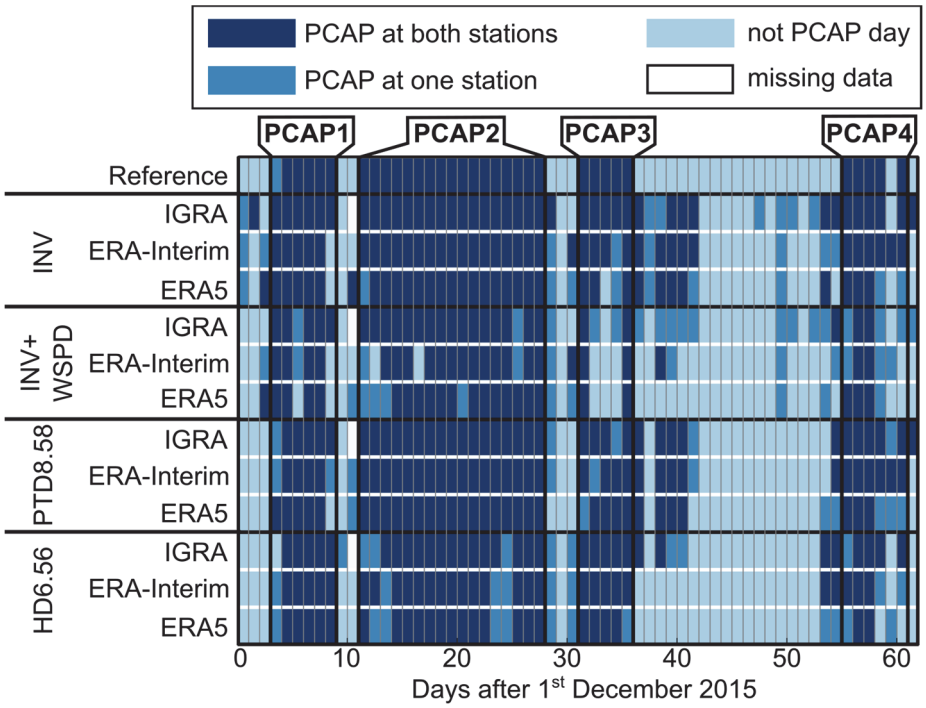

Fig. 11. The temporal distribution of PCAP days according to different definitions using different databases for two stations (Budapest and Szeged, Hungary) between December 1, 2015 and January 31, 2016. The reference is based on the Daily Weather Reports of the HMS and the vertical distribution of air temperature.

4.2.1. Numerical methods vs. reference

In general, the four PCAP periods can be identified using any of the methods (*Fig. 11*). During PCAP conditions, the values of HD usually exceed the determined threshold (*Fig. 12*) even during the special PCAP3 period. Some PCAP days were indicated falsely before PCAP4 using INV and INV+WSPD method. These are caused by thin inversion layers (~80-90 m thick), not PCAP-like inversions. PCAP3 period is almost fully or partly missing when the INV+WSPD method is used. The explanation for INV+WSPD's underperformance is the unusual high wind speeds during this period (*Fig. 10*). This suggests that wind affects PCAPs less in large basins than in smaller valleys. This emphasizes the need for careful consideration of the method and meteorological parameters to be used over different terrains.

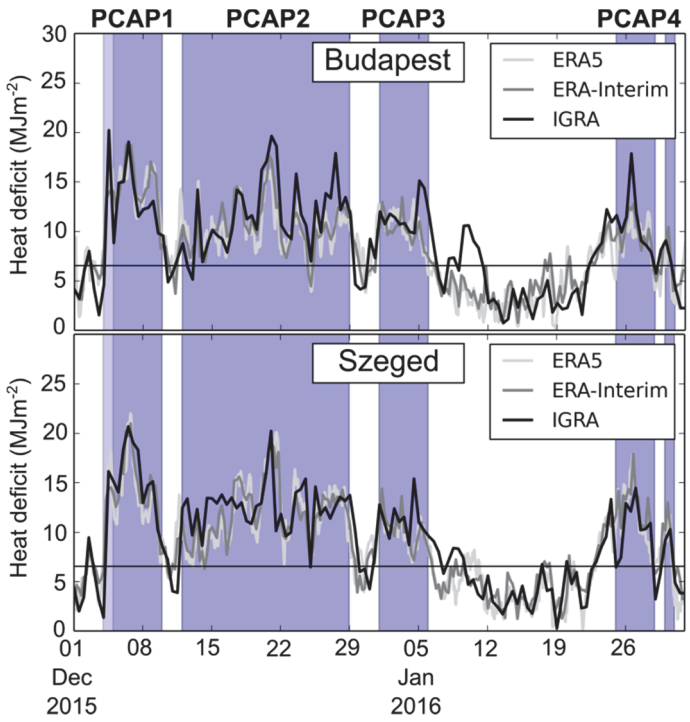

Fig. 12. Heat deficit in Budapest (top) and Szeged (bottom) between December 2015 and January 2016. The threshold used to define PCAP conditions is indicated by a horizontal line. The reference PCAP days are also indicated (shaded areas; darker: PCAP present at both stations, light: it is present only at Budapest).

PCAP3 is extended when INV or PTD8.58 methods are used with any of the databases. The inversion caused by a warm front described in Section 4.1 was indicated by PTD, but the values of the HD were below the given threshold. This situation is particularly apparent when reanalysis data was used.

4.2.2. Measurements vs. reanalyses

The most obvious difference between measurements and reanalyses can be observed in case of PCAP3 using HD6.56 method (*Fig. 11*). The extension of PCAP3 is present when IGRA measurements are used. These false detections are not found with reanalysis data. This difference probably comes from the difference between the databases: measurements are station data (representing single point-like location), but reanalyses contain gridded data (the values are averaged over entire grid cells). The size of the grid cells of ERA-Interim and ERA5 is approximately 6000 km^2 and 1000 km^2, respectively. The vertical resolutions also differ: reanalyses offer data on fixed pressure levels with coarser vertical resolution than the measurements. Therefore, strong local inversions may be missing from reanalyses. This leads to a decrease in HD. The days of the extension after PCAP3 were not PCAP days according to the reference. However, they were PCAP days at least over one station according to the measurements.

Besides the differences in spatial resolution, the temporal resolution also affects the results. For instance, the end of PCAP1 can illustrate this well. When only two measurements are used daily (with a difference of 12 h between them), the PCAP dissipates later than in the case of 6 hourly or 1 hourly reanalyses data. In this case, the IGRA measurements are more similar to the reference than reanalyses. Note that the reference data series was created using IGRA in addition to the DWR. The reference data series has some uncertainty in dissipation time of PCAPs due to the temporal resolution of IGRA and DWR. It means that the reanalyses can be more representative than the measurements because of their finer temporal resolution.

The radiosonde measurements are used in the reanalyses through data assimilation, therefore, the vertical temperature profiles of the three databases at 00 and 12 UTC (when radiosonde measurements are performed) should be similar to each other. However, large differences can be seen in *Fig. 13* between the vertical temperature profiles of measurements and reanalyses. The data assimilation method and the spatial resolution could result in this difference. High correlations between the time series of HD are also expected. The Spearman's correlation coefficients of the two-month-long HD time series between ERA-Interim and IGRA are slightly higher (0.86 and 0.87 at Budapest and Szeged, respectively) than between ERA5 and IGRA (0.81 and 0.84 at Budapest and Szeged, respectively).

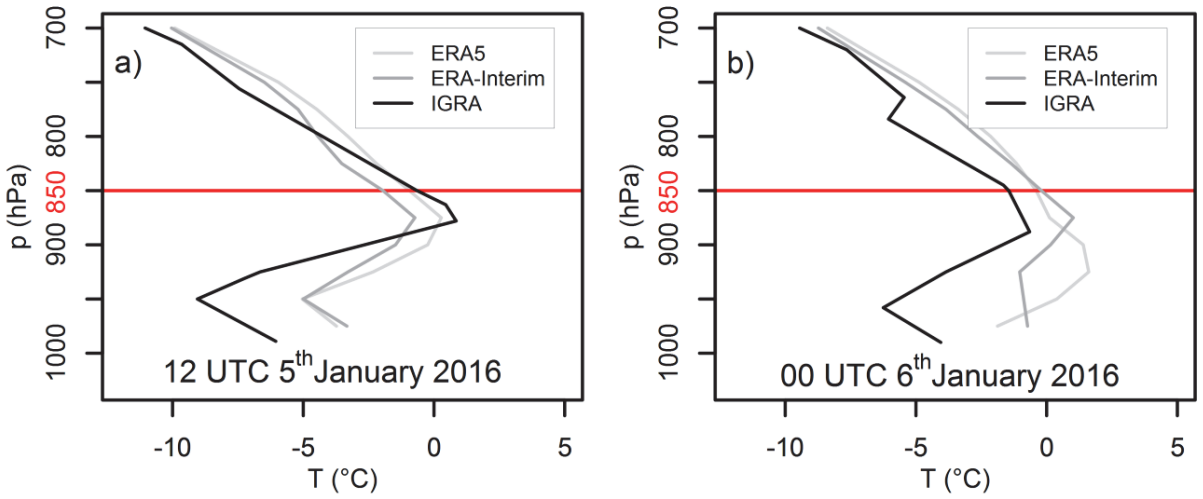

Fig. 13. Vertical distribution of atmospheric temperature at Budapest at a) 12 UTC, January 5, 2016 and b) 00 UTC, January 6, 2016 according to radiosonde measurements (black), ERA-Interim (dark grey), and ERA5 (light grey) databases.

4.2.3. ERA-Interim vs. ERA5

The different temporal resolution causes differences between the results of the two reanalyses, too. In general, the results of ERA-Interim and ERA5 are similar to each other when using PTD8.58 and HD6.56 method (*Fig. 11*). In general, the vertical distributions of atmospheric temperature based on ERA-Interim and ERA5 are also more similar to each other than the radiosonde measurements (e.g., 12 UTC, January 5, 2016, *Fig. 13a*). The Spearman's correlation coefficient of the two-month-long HD time series between ERA-Interim and ERA5 is 0.93 and 0.95 at Budapest and Szeged, respectively. Despite the high values, there are differences between the results of the two reanalyses. For example, the dissipation of PCAP3 is predicted one day earlier at Budapest when using HD6.56 method with ERA5 data (the value of HD fell below the threshold at 20 UTC, January 5). The top of the inversion was higher in ERA-Interim than in ERA5 at 00 UTC, January 6 (*Fig. 13b*). Therefore, HD was lower in ERA5 (5.8 MJm^{-2}) than in ERA-Interim (7.1 MJm^{-2}) and fell below the 6.56 MJm^{-2} threshold.

Additionally, there are differences between the two reanalyses during PCAP4. The results of ERA-Interim are closer to the IGRA measurements and are more similar to the reference than ERA5 results. This is probably caused by the different spatial resolution**:** ERA-Interim has coarser spatial resolution than ERA5, so it is more representative for a larger area and it fits better to the reference (it is difficult to delimit the exact location of the station using DWR, see Section 3.1).

4.2.4. Comparing the identifications at the two test locations

There is just one day (December 4, 2015) when the PCAP was present only at Budapest according to the reference database. However, the results of numerical PCAP identification differ at the two stations on several (5–18) days (*Fig. 11*). Most of the differences (10–18 days) are present using the INV+WSPD method because, in general, the daily maximum wind gusts were greater at Szeged than in Budapest (*Fig. 10*). The least differences (5–7 days) are present using the PTD8.58 method. Therefore, this method seems to be the most location-independent. Besides, numerical methods are applied to well-defined areas (e.g., precise location, grid cell) in contrast to the reference, in which the areas around the stations are identified from context. Because of the distance between the two stations, different results can be expected. This emphasizes the importance of involving more stations and using data covering larger area to determine CAPs extended to large basins. The method of defining the reference PCAP days data series is also suitable to describe extended PCAPs.

4.3. Evaluation of errors

POM, POFD, and ERR are shown in *Fig. 14*. In general, the values of POFD are higher than POM almost in all cases. It means that the methods rather overestimate the number of PCAP-like days. High values of POM are present when the INV+WSPD method was used, because wind speeds were high during PCAP3 and towards the end of PCAP4 (*Fig. 10*). An outstanding value of POFD is found in case of INV method because of thin inversion layers. PTD8.58 is the other method, which substantially overestimates the number of PCAP days.

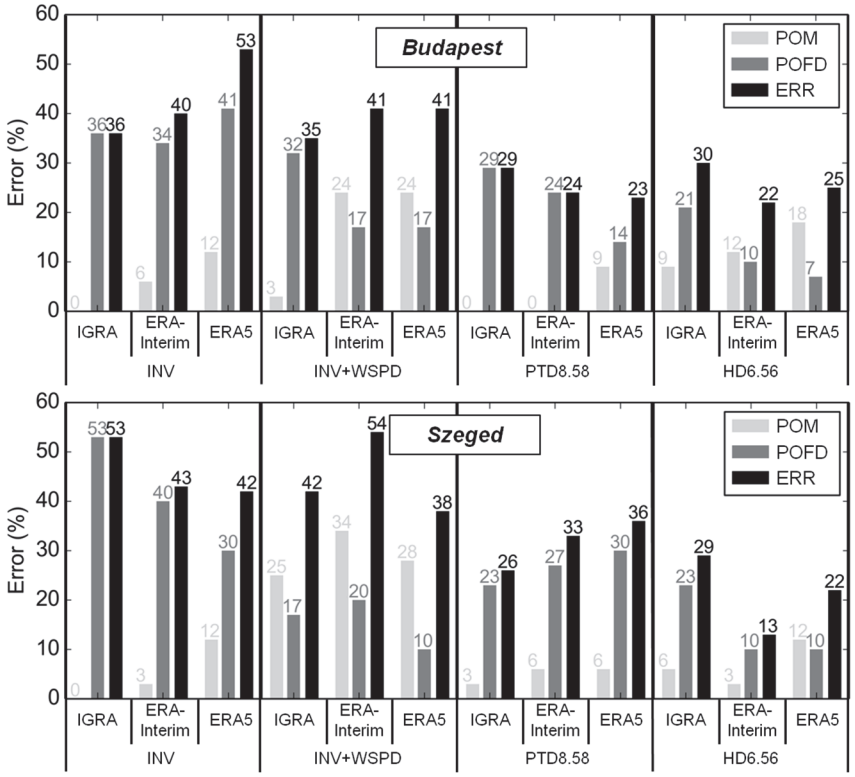

Fig. 14. Probability of miss (POM) and probability of false detection (POFD), and sum of them (ERR) at Budapest (top) and Szeged (bottom).

4.3.1. Differences in the errors of the different numerical methods

In general, the results are similar at Budapest and Szeged, when the PTD8.58 or the HD6.56 methods were used to identify PCAPs (*Fig. 14*). Additionally, POM values are similar also when using the INV method. There are larger differences between the results of the two stations when applying INV or INV+WSPD method. Consequently, it is recommended to use the PTD8.58 or (more preferably) the HD6.56 method to identify PCAPs over large basins rather than inversion-based methods.

4.3.2. Evaluation of average total error

The value of ERR averaged over the stations is shown in *Fig. 15* for the different methods. The lowest average ERR is produced by using HD6.56 method (24%), and the PTD8.58 method results in the second lowest value (29%). When the two gridded databases are compared, the use of ERA-Interim as source data results in lower average ERR (18%) than the use of ERA5 (24%) in case of HD6.56 method. According to these results, HD6.56 definition is preferred for the local identification of PCAPs using ERA-Interim data.

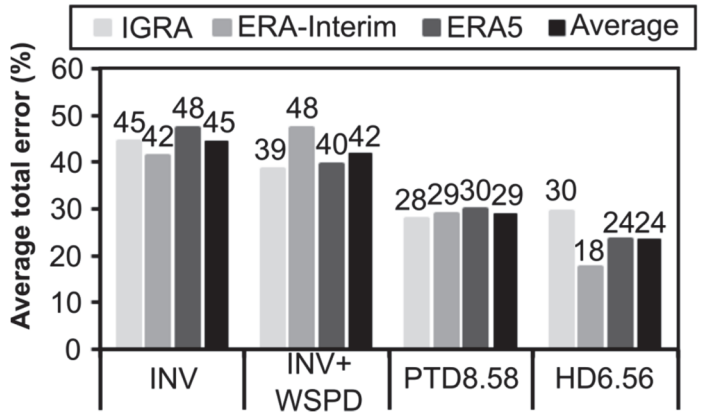

Fig. 15. Value of average total error for different numerical methods.

5. Summary and conclusions

In this study, it was examined how effective the existing numerical CAP definitions are in cases of PCAP events in the Great Hungarian Plain. Four different methods were compared to the reference and to each other during two consecutive winter months (December 2015 and January 2016). The considered methods have been adapted from other authors who examined CAPs in small valleys and basins. In order to determine which method performs better, a reference PCAP days data series was created using the regular DWRs of the HMS and radiosonde measurements. After applying the numerical methods to the various datasets, the probability of misses and false detections and the sum of them (total error) were calculated.

On the basis of the presented analysis, the following conclusions can be drawn:

(1) Wind affects PCAPs less in large basins than in smaller valleys.

(2) The lowest value of total error is produced by using the HD6.56 method (heat deficit below 850 hPa is larger than 6.56 MJm^{-2}), which highlights the potential further use of this method in numerical-based objective definition of PCAP.

(3) From the three examined databases, the use of ERA-Interim data yielded the lowest value of total error when it was used with the HD6.56 method.

Overall, HD6.56 definition is preferred for the local identification of PCAPs using gridded analyses dataset providing that the reference PCAP days is selected according to the description in Section 3.1. Results obtained by using PTD method are also promising, because the errors are only slightly higher than in case of HD6.56.

The present study is not exhaustive and has limitations: (i) textual Daily Weather Reports were (also) used to determine the reference PCAP days data series, making the study partly subjective; (ii) we examined only a two-month-period; (iii) we processed the data of only 2 stations, because there are only two radio sounding stations in Hungary; (iv) the measures used do not take into account cloud formation (or at least the value of relative humidity). One possibility to improve the predictions can be if the measures used in this study were combined with other variables (e.g., relative humidity, tendency of mean sea level pressure, etc.) so that, for example, the inversion caused by the warm front and the inversion present in the PCAPs could be distinguished (see days after PCAP3, Section 4.2.1). Automation of the procedure of obtaining the reference set of PCAP days is possible and is planned using, e.g., SYNOP telegrams and radiosonde data. This would serve either as an alternative method for determining PCAP conditions objectively, and would also make it possible to extend this study in time and space (i.e., to more locations) in order to refine the numerical definitions examined in this work. The numerical definition(s) could be used in synoptic-climatological research and air quality studies (e.g., *Haszpra et al*., 2019) as well as by weather forecasters during post-processing of numerical weather prediction models. Another possible utilization of the suggested numerical method is forecasting the outages in the production of green energy. Solar and wind energy production is heavily influenced by the weather. Having a foggy or cloudy PCAP for several days, or even weeks, with windless weather can prevent the use of these renewable sources. This is why it is important to know the frequency over time and average length of PCAPs, and how these features are likely to change in the future.

Acknowledgements: This work was supported by the Széchenyi 2020 programme, the European Regional Development Fund and the Hungarian Government via the AgroMo project [grant number GINOP-2.3.2-15-2016-00028]; the ELTE Institutional Excellence Program [grant number TKP2020-IKA-05] financed by the Hungarian Ministry of Human Capacities; and the Hungarian National Research, Development and Innovation Fund [grant numbers K-120605 and K-129162]. This study is a contribution to the PannEx Regional Hydroclimate Project of the World Climate Research Programme (WCRP) Global Energy and Water Exchanges (GEWEX) Project.

The analysis used modified Copernicus Climate Change Service information (ERA-Interim and ERA5 data) [2019].

The first author of this paper would like to say thank to *András Zénó Gyöngyösi* for his help and guidance in the world of cold air pools.

References

Baasandorj, M., Hoch, S.W., Bares, R., Lin, J.C., Brown, S.S., Millet, D.B., Martin, R., Kelly, K., Zarzana, K.J., Whiteman, C.D., Dube, W.P., Tonnesen, G., Jaramillo, I.C., and *Sohl, J.,* 2017: Coupling between Chemical and Meteorological Processes under Persistent Cold-Air Pool Conditions: Evolution of Wintertime PM2.5 Pollution Events and N2O5 Observations in Utah's Salt Lake Valley. E*nviron. Sci. Technol. 51*, 5941–5950. https://doi.org/10.1021/acs.est.6b06603

Chachere, C.N. and *Pu, Z.,* 2016: Connections Between Cold Air Pools and Mountain Valley Fog Events in Salt Lake City. *Pure Appl. Geophys. 173*, 3187–3196. https://doi.org/10.1007/s00024-016-1316-x

Chemel, C., Arduini, G., Staquet, C., Largeron, Y., Legain, D., Tzanos, D., and *Paci, A*., 2016: Valley heat deficit as a bulk measure of wintertime particulate air pollution in the Arve River Valley. *Atmos. Environ. 128*, 208–215. https://doi.org/10.1016/j.atmosenv.2015.12.058

Conangla, L., Cuxart, J., Jiménez Maria, A., Martínez-Villagrasa, D., Miró Josep, R., Tabarelli, D., and *Zardi, D*., 2018: Cold-air pool evolution in a wide Pyrenean valley. I*nt. J. Climatol. 38*, 2852–2865. https://doi.org/10.1002/joc.5467

Cuxart, J., Yagüe, C., Morales, G., Terradellas, E., Orbe, J., Calvo, J., Fernández, A., Soler, M.R., Infante, C., Buenestado, P., Espinalt, A., Joergensen, H.E., Rees, J.M., Vilá, J., Redondo, J.M., Cantalapiedra, I.R., and *Conangla, L*., 2000: Stable Atmospheric Boundary-Layer Experiment in Spain (SABLES 98): A Report. *Bound.-Layer Meteorol. 96*, 337–370. https://doi.org/10.1023/A:1002609509707

Dee, D.P., Uppala, S.M., Simmons, A.J., Berrisford, P., Poli, P., Kobayashi, S., Andrae, U., Balmaseda, M.A., Balsamo, G., Bauer, P., Bechtold, P., Beljaars, A.C.M., van de Berg, L., Bidlot, J., Bormann, N., Delsol, C., Dragani, R., Fuentes, M., Geer, A.J., Haimberger, L., Healy, S.B., Hersbach, H., Hólm, E.V., Isaksen, L., Kållberg, P., Köhler, M., Matricardi, M., McNally, A.P., Monge-Sanz, B.M., Morcrette, J.-J., Park, B.-K., Peubey, C., de Rosnay, P., Tavolato, C., Thépaut, J.-N., and *Vitart, F*., 2011: The ERA-Interim reanalysis: configuration and performance of the data assimilation system. *Quart. J. Roy. Meteorol. Soc. 137*, 553–597. https://doi.org/10.1002/qj.828

Deng, X., Cao, W., Huo, Y., Yang, G., Yu, C., He, D., Deng, W., Fu, W., Ding, H., Zhai, J., Cheng, L., and *Zhao, X*., 2019: Meteorological conditions during a severe, prolonged regional heavy air pollution episode in eastern China from December 2016 to January 2017. *Theor. Appl. Climatol. 135*, 1105–1122. https://doi.org/10.1007/s00704-018-2426-4

Durre, I., Vose, R.S., and *Wuertz, D.B.*, 2006: Overview of the Integrated Global Radiosonde Archive. *J. Climat. 19*, 53–68. https://doi.org/10.1175/JCLI3594.1

DWR website: Daily Weather Reports of the Hungarian Meteorological Service. (in Hungarian) https://www.met.hu/idojaras/aktualis_idojaras/napijelentes/ (accessed 4 April 2019)

ERA5 dataset: Copernicus Climate Change Service (C3S), 2017: ERA5: Fifth generation of ECMWF atmospheric reanalyses of the global climate. Copernicus Climate Change Service Climate Data Store (CDS), accessed 18 February 2019, available from https://cds.climate.copernicus.eu/cdsapp#!/home

ERA-Interim dataset: European Centre for Medium-range Weather Forecast (ECMWF), 2011: The ERA-Interim reanalysis dataset, Copernicus Climate Change Service (C3S), accessed 18 February 2019, available from https://www.ecmwf.int/en/forecasts/datasets/archive-datasets/reanalysis-datasets/era-interim

Haszpra, L., Ferenczi, Z., and *Barcza, Z.*, 2019: Estimation of Greenhouse Gas Emission Factors Based on Observed Covariance of CO_2, CH_4, N_2O and CO Mole Fractions. *Environ. Sci. Eur. 31*, 95. https://doi.org/10.1186/s12302-019-0277-y

Hersbach, H., Bell, W., Berrisford, P., Horányi, A., Muñoz Sabater, J., Nicolas, J., Radu, R., Schepers, D., Simmons, A., Soci, C., and *Dee, D.*, 2019. Global reanalysis: goodbye ERA-Interim, hello ERA5. *ECMWF Newsl. 159*, 17–24. https://doi.org/10.21957/vf291hehd7

IGRA dataset: *Durre, I.; Xungang, Y.; Vose, R. S.; Applequist, S.;* and *Arnfield, J.*, 2016: Integrated Global Radiosonde Archive (IGRA), Version 2. [Derived]. NOAA National Centers for Environmental Information. http://doi.org/10.7289/V5X63K0Q (accessed 14 October 2018).

Iijima, Y. and *Shinoda, M.*, 2000: Seasonal changes in the cold-air pool formation in a subalpine hollow, central Japan. *Int. J. Climatol. 20*, 1471–1483. https://doi.org/10.1002/1097-0088(200010)20:12<1471::AID-JOC554>3.0.CO;2-6

ISD dataset: NOAA National Centers for Environmental Information, 2001: Global Surface Hourly [Integrated Surface Global Hourly data]. NOAA National Centers for Environmental Information, accessed 26 July 2019, available from https://data.nodc.noaa.gov/cgi-bin/iso?id=gov.noaa.ncdc:C00532

Kahl, J.D., 1990: Characteristics of the low-level temperature inversion along the Alaskan Arctic coast. *Int. J. Climatol. 10*, 537–548. https://doi.org/10.1002/joc.3370100509

Kahl, J.D., Serreze, M.C., and *Schnell, R.C.,* 1992. Tropospheric low-level temperature inversions in the Canadian Arctic. *Atmosphere-Ocean 30,* 511–529. https://doi.org/10.1080/07055900.1992.9649453

Lareau, N.P., Crosman, E., Whiteman, C.D., Horel, J.D., Hoch, S.W., Brown, W.O.J., and *Horst, T.W.,* 2013. The Persistent Cold-Air Pool Study. *Bull. Amer. Meteorol. Soc. 94*, 51–63. https://doi.org/10.1175/BAMS-D-11-00255.1

Largeron, Y. and *Staquet, C.*, 2016a: Persistent inversion dynamics and wintertime PM10 air pollution in Alpine valleys. *Atmos. Environ. 135*, 92–108. https://doi.org/10.1016/j.atmosenv.2016.03.045

Largeron, Y. and *Staquet, C.*, 2016b: The Atmospheric Boundary Layer during Wintertime Persistent Inversions in the Grenoble Valleys. Front. *Earth Sci. 4*, e40. https://doi.org/10.3389/feart.2016.00070

Llasat, M.C. and *Puigcerver, M.*, 1990: Cold air pools over Europe. *Meteorol. Atmospheric Phys. 42*, 171–177. https://doi.org/10.1007/BF01314823

Nurmi, P., 2003: Recommendations on the verification of local weather forecasts. *ECMWF Tech. Memo. 430*, 19. https://doi.org/10.21957/y1z1thg5l

Price, J.D., Vosper, S., Brown, A., Ross, A., Clark, P., Davies, F., Horlacher, V., Claxton, B., McGregor, J.R., Hoare, J.S., Jemmett-Smith, B., and *Sheridan, P.,* 2011: COLPEX: Field and Numerical Studies over a Region of Small Hills. *Bull. Amer. Meteorol. Soc. 92*, 1636–1650. https://doi.org/10.1175/2011BAMS3032.1

Reeves, H.D., Elmore, K.L., Manikin, G.S., and *Stensrud, D.J.,* 2011: Assessment of Forecasts during Persistent Valley Cold Pools in the Bonneville Basin by the North American Mesoscale Model. *Weather Forecast 26*, 447–467. https://doi.org/10.1175/WAF-D-10-05014.1

Reeves, H.D. and *Stensrud, D.J.*, 2009: Synoptic-Scale Flow and Valley Cold Pool Evolution in the Western United States. *Weather Forecast 24*, 1625–1643. https://doi.org/10.1175/2009WAF2222234.1

Smith, A., Lott, N., and *Vose, R.*, 2011: The Integrated Surface Database: Recent Developments and Partnerships. *Bull. Amer. Meteorol. Soc. 92*, 704–708. https://doi.org/10.1175/2011BAMS3015.1

Tóth, P., 1984: Parametrizáció bevezetése hideg légpárnák keletkezésének és feloszlásának analízise céljából.) Országos Meteorológiai Szolgálat, Meteorológiai Tanulmányok, 51. (In Hungarian)

Vitasse, Y., Klein, G., Kirchner, J.W., and *Rebetez, M.*, 2017: Intensity, frequency and spatial configuration of winter temperature inversions in the closed La Brevine valley, Switzerland. *Theor. Appl. Climatol. 130*, 1073–1083. https://doi.org/10.1007/s00704-016-1944-1

Whiteman, C.D., Bian, X., and *Zhong, S.,* 1999: Wintertime Evolution of the Temperature Inversion in the Colorado Plateau Basin. *J. Appl. Meteorol. 38*, 1103–1117. https://doi.org/10.1175/1520-0450(1999)038<1103:WEOTTI>2.0.CO;2

Whiteman, C.D., Hoch, S.W., Horel, J.D., and *Charland, A.*, 2014: Relationship between particulate air pollution and meteorological variables in Utah's Salt Lake Valley. *Atmos. Environ. 94*, 742–753. https://doi.org/10.1016/j.atmosenv.2014.06.012

Whiteman, C.D., Muschinski, A., Zhong, S., Fritts, D., Hoch, S.W., Hahnenberger, M., Yao, W., Hohreiter, V., Behn, M., Cheon, Y., Clements, C.B., Horst, T.W., Brown, W.O.J., and *Oncley, S.P.,* 2008: Metcrax 2006: Meteorological Experiments in Arizona's Meteor Crater. *Bull. Amer. Meteorol. Soc. 89*, 1665–1680. https://doi.org/10.1175/2008BAMS2574.1

Whiteman, C.D., Zhong, S., Shaw, W.J., Hubbe, J.M., Bian, X., and *Mittelstadt, J.,* 2001: Cold Pools in the Columbia Basin. *Weather Forecast 16,* 432–447. https://doi.org/10.1175/1520-0434(2001)016<0432:CPITCB>2.0.CO;2

Wolyn, P.G. and *McKee, T.B*., 1989: Deep Stable Layers in the Intermountain Western United States. *Mon. Weather Rev. 117,* 461–472. https://doi.org/10.1175/1520-0493(1989)117<0461:DSLITI>2.0.CO;2

Yu, L., Zhong, S., and *Bian, X*., 2017: Multi-day valley cold-air pools in the western United States as derived from NARR. *Int. J. Climatol. 37*, 2466–2476. https://doi.org/10.1002/joc.4858